AIP | Conference Proceedings

Modulational instability of microbubbles surface modes

Serge Dos Santos, Víctor Sánchez-Morcillo, Noé Jiménez, André-Pierre Abellard, and Ayache Bouakaz

Citation: AIP Conf. Proc. **1433**, 311 (2012); doi: 10.1063/1.3703195
View online: http://dx.doi.org/10.1063/1.3703195
View Table of Contents: http://proceedings.aip.org/dbt/dbt.jsp?KEY=APCPCS&Volume=1433&Issue=1
Published by the American Institute of Physics.

Related Articles

Time-resolved monitoring of cavitation activity in megasonic cleaning systems
Rev. Sci. Instrum. 83, 034904 (2012)

Laser-nucleated acoustic cavitation in focused ultrasound
Rev. Sci. Instrum. 82, 044902 (2011)

When sound slows down bubbles
Phys. Fluids 22, 041703 (2010)

The acoustic response from individual attached and unattached rigid shelled microbubbles
Appl. Phys. Lett. 93, 223906 (2008)

Optical observation of lipid- and polymer-shelled ultrasound microbubble contrast agents
Appl. Phys. Lett. 84, 631 (2004)

Additional information on AIP Conf. Proc.

Journal Homepage: http://proceedings.aip.org/
Journal Information: http://proceedings.aip.org/about/about_the_proceedings
Top downloads: http://proceedings.aip.org/dbt/most_downloaded.jsp?KEY=APCPCS
Information for Authors: http://proceedings.aip.org/authors/information_for_authors

ADVERTISEMENT



Downloaded 25 May 2012 to 156.111.111.124. Redistribution subject to AIP license or copyright; see http://proceedings.aip.org/about/rights_permissions

Modulational Instability of Microbubbles Surface Modes

Serge Dos Santos*, Víctor Sánchez-Morcillo†, Noé Jiménez†, André-Pierre Abellard ** and Ayache Bouakaz**

*Centre - Val de Loire Université, ENI Val de Loire, Unité Mixte de Recherche "Imagerie et Cerveau", INSERM U930 - CNRS ERL 3106, Rue de la Chocolaterie, BP3410, 41034 Blois cedex, FRANCE
†Departamento de Fisica Aplicada, Instituto de Investigación para la Gestión, Integrada de las Zonas Costeras (IGIC), Universidad Politecnica de Valencia, c/ Paranimf nž 1, 46730 Grao de Gandia, SPAIN
**Unité Mixte de Recherche " Imagerie et Cerveau " INSERM U930 - CNRS ERL 3106, Université François Rabelais, Bâtiment B1A, 1er Étage, CHRU Bretonneau 2 boulevard Tonnellé, 37044 Tours Cedex, FRANCE

Abstract. Starting from the continuous Marmottant model[1], for the vibration of the bubble radius R(t), and a discrete nonlinear model of the discretized radius with periodic boundary conditions and nonlinear coupling between surface modes, MI in bubbles is investigated numerically. After a first step of Symmetry Analysis[2] applied to the nonlinear equations associated to the models, invariant properties allow an identification of dimensionless similarity variables that link both continuous and discrete models. Thanks to this similarity analysis, the bubble can be studied with a macroscopic mechanical 1D ring chain (diameter =73 cm) using N=48 nonlinearly coupled pendulum of mass m=6g and length =3.2cm with periodic conditions. The second step consists in studying numerically the MI criterion versus the amplitude of external field applied to the bubble. The analysis and the experiments reveals the existence of Intrinsic Localized Modes (ILMs), similar to those found in other more generic systems of nonlinearly vibratory lattices. The observation of ILM in 1D chain of coupled oscillators[3, 4], presenting many similarities with the discrete bubble model, showed to play a role in creating spatio-temporal localized excitations leading to the breaking of the bubble. In our periodic pendulum lattice apparatus describing the macroscopic equivalence of the bubble, the system parametrically driven at 5.4 Hz presents subharmonic behavior and localized modes oscillating at 2.7 Hz. Versus the amplitude and the frequency of the driving, the mechanical ring presents parametric instability surface modes and localized modes oscillating at subharmonics of the parametric excitation.

Keywords: Ultrasound Contrast Agents, Bubble oscillation, Parametric instability
PACS: 43.25.Yw, 43.35.Ei, 43.80.Gx, 43.35.Wa

INTRODUCTION

Microbubble surface modes appear when contrast agents are insonified with specific ultrasound pulses[5]. In this case, the radius is a space-dependent function which can be expanded on the basis of spherical harmonics describing the spatial vibrational modes of the bubble. Modulational Instability (MI) is an instability of the vibration modes in nonlinear systems induced by an external driving, and can be physically interpreted as a nonlinear four-wave (or four-mode) mixing process. The objective is to study microbubbles surface modes which appears when UCA are driven by ultrasound and exhibit shape-unstable behavior caracterized by parametric instability. As the parametric instability increases, the spherically symmetric wall oscillation ($R(t) = R_0 + r(t)$) is no more present and an unstable behavior coming from breathing mode appears and some spherical modes are growing resulting from symmetry breaking : $R(t) \rightsquigarrow R(t, \theta, \phi)$. Bubbles are used as contrast agent in medical ultrasound imaging and to carry some drug to special locations. Our interest in this study would be to determine the external acoustical pressure on a bubble to a given excitation frequency for a specific surface mode. Microbubbles submit to high powers ultrasound generate a radial oscillation mode. Which one can power up surface waves by instabilities at the surface layer. They are called too surfaces modes. This surface mode can be analytically described as a linear composition of spherical harmonics [7] and [8]. We purpose to you to link this phenomenon as the modulational instability. Modulational instability (ref Observation of modulational.) is the observation of instability into vibration mode in non linear system. System who has been excited by an external driving.Like the external acoustical for the bubble. Assuming that the Hamiltonian formalism of the nonlinear bubble dynamics[6], on can generalize the expansion of the radius in a series of spherical harmonics with

International Congress on Ultrasonics
AIP Conf. Proc. 1433, 311-314 (2012); doi: 10.1063/1.3703195
© 2012 American Institute of Physics 978-0-7354-1019-0/$30.00

Downloaded 25 May 2012 to 156.111.111.124. Redistribution subject to AIP license or copyright; see http://proceedings.aip.org/about/rights_permissions

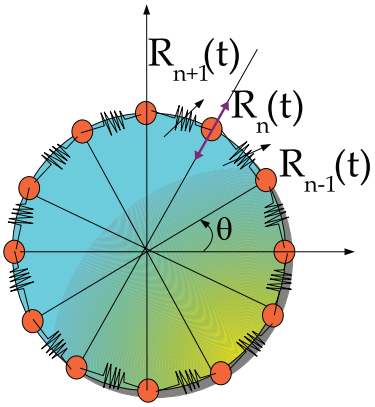


FIGURE 1. Simplified model of the bubble with discrete radius $R(t,\theta,\phi) \rightsquigarrow R(t,\theta) \rightsquigarrow R_n(t)$. Each particle produce a radial evolution $R_n(t)$ depending on the substrat potential given by the nonlinear characteristics plotted in Fig.**??**(b) and a linear coupling depending on the first neighbors $f(R_{n-1}(t),R_n(t),R_{n+1}(t))$

$$R(t) \rightsquigarrow R(t,\theta,\phi) = R(t) + \varepsilon \sum_{l=0}^{\infty} \sum_{m=-l}^{l} a_l(t) Y_l^{(m)}(\theta,\phi). \tag{1}$$

The monopole pulsation ($l=0$) is characterized by the resonance frequency $\omega_0^2 = \frac{3}{\rho_l R_0^2} K_V = \frac{3}{\rho_l R_0^2}\left(\kappa P_{atm} + \frac{2(3\kappa-1)\sigma}{R_0}\right)$, the dipole mode ($l=1$) corresponds to translational motions (displacement of the bubble center of mass), and shape oscillations ($l>2$) are characterized by

$$\omega_l^2 = (l-1)(l+1)(l+2)\frac{\sigma}{\rho R_0^3}. \tag{2}$$

BUBBLE MODELING

Marmottant models [1] stand on the Rayleigh-Plesset with some boundary conditions. The boundary is the fact that he takes in charge the surface tension dependence $\sigma(R)$. He treats the surface tension in three cases : buckled bubbles, elastics bubbles and ruptured bubbles. The last one can be seen like free bubbles. It could be considered like bubbles without shell in their properties. The boundary condition on the Rayleigh Plesset equation is

$$P_g(t) - P_l(t) = \frac{2\sigma(R)}{R} + 4\mu\frac{\dot{R}}{R} + 4\kappa_s\frac{\dot{R}}{R^2} \tag{3}$$

By taking in Rayleigh-plesset, you obtain the Marmottant's model, who stand on this equation :

$$\begin{aligned} &\rho_l\left(R\tfrac{\partial^2 R}{\partial t^2} + \tfrac{3}{2}\left(\tfrac{\partial R}{\partial t}\right)^2\right) \\ &= \left(P_0 + \tfrac{2\sigma(R_0)}{R_0}\right)\left(\tfrac{R}{R_0}\right)^{-3\kappa}\left(1 - \tfrac{3\kappa}{c}\tfrac{\partial R}{\partial t}\right) \\ &-P_0 - 2\tfrac{\sigma(R)}{R} - \tfrac{4\mu\frac{\partial R}{\partial t}}{R} - \tfrac{4\kappa_s\frac{\partial R}{\partial t}}{R^2} - P_{ac}(t) \end{aligned} \tag{4}$$

After rewritting equation, one can explain :

$$\rho_l\left(R\ddot{R} + \frac{3}{2}\dot{R}^2\right) - \left(P_0 + \frac{2\sigma(R_0)}{R_0}\right)\left(\frac{R}{R_0}\right)^{-3\kappa}\left(1 - \frac{3\kappa}{c}\dot{R}\right) + P_0 + 2\frac{\sigma(R)}{R} + \frac{4\mu\dot{R}}{R} + \frac{4\kappa_s\dot{R}}{R^2} = -P_{ac}(t) \tag{5}$$

Downloaded 25 May 2012 to 156.111.111.124. Redistribution subject to AIP license or copyright; see http://proceedings.aip.org/about/rights_permissions



FIGURE 2. Macroscopic spherical pendulum chain with the following parameters $N = 48$, $R_0 = 36.5cm$, $m = 6g$ and $h = 15cm$(right), $h = 3cm$(left). The parametric excitation is driven at frequency $f_e = 2.57\ Hz$ and the spherical mode $Y_{l=8}^{(m)}$ appears. The parametric excitation is driven at $f_e = 4.5\ Hz$ and the localized mode appears and oscillation of the single particule is around $f_{osc} = \frac{f_e}{2}$.

where bubble parameters are $\rho_l, \sigma, \kappa, c, \mu, \kappa_s$. With an external driving is $P = P_0 + P_{ac}(t)$, linearization consist in assuming $R(t) = R_0 + \varepsilon r(t)$, and $\sigma(R) = \sigma(R_0) + 2\varepsilon\kappa\left(\frac{R}{R_0} - 1\right)$. In this case, it can be shown that $\ddot{r}(t) + 2\gamma\dot{r}(t) + \omega_0^2 r(t) = -\frac{P_{ac}(t)}{\rho_l R_0^2}$, where ω_0 is given by $\omega_0^2 = \frac{3}{\rho_l R_0^2} K_V = \frac{3}{\rho_l R_0^2}\left(\kappa P_{atm} + \frac{2(3\kappa-1)\sigma}{R_0}\right)$.

Assuming classical values for physical parameters of the bubble, one have

$$f_0[MHz].R_0[\mu m] \simeq 3 \tag{6}$$

The similarity property can be written $f_0[Hz].R_0[m] \simeq 3$ and explain the typical sizes chosen for the macroscopic experiment with coupled pendulum. Using Prosperetti Model with spherical harmonics $Y_l^{(m)}(\theta,\phi)$, bubble oscillation is then given by $\ddot{a}_l(t) + 2\gamma\dot{a}_l(t) + \omega_l^2 a_l(t) = 0$, where ω_l is given by $\omega_l^2 = (l-1)(l+1)(l+2)\frac{\sigma}{\rho R_0^3}$. If spherical mode is unstable, *i.e.* $R(t) \rightsquigarrow R(t,\theta)$, Modulational Instability (MI) appears and localized behavior is observed when $\omega_{ext} = 1.92 f_0$ as shown in Fig.**??**.

EXPERIMENT AND SIMULATIONS

The hypothesis are the following. We assume that

$$R(t,\theta,\phi) \rightsquigarrow R(t,\theta) \rightsquigarrow R_n(t) \tag{7}$$

where $R_n(t)$ is the position of the radius bubble at angle $\theta = n\theta_0$, $\theta_0 = 2\pi/N$ being the sampling step of the θ-discretization ($n = 0, \ldots, N-1$). The following model is then derived

$$\ddot{R}_n(t) + \sin\left(R_n(t)\right)\left[\omega_0^2 + \eta\cos(2\omega_{ext}t)\right] + \gamma R_n'(t) = f\left(R_{n-1}(t) - 2R_n(t) + R_{n+1}(t)\right) \tag{8}$$

with the periodic condition $R_N(t) = R_0(t)$. As shown if the fig.2, the $N = 8$ mode is observed numerically. Experiments have been conducted[1] assuming Prosperetti Model with spherical harmonics $Y_l^{(m)}(\theta,\phi)$. The hypothesis are the following. We assume that

$$R(t) \rightsquigarrow R(t,\theta,\phi) = R(t) + \varepsilon \sum_{(l,m)} a_l(t) Y_l^{(m)}(\theta,\phi), \tag{9}$$

[1] See `http://ultrasons-inserm.med.univ-tours.fr/aTelecharger/sDos/ICU-Gdansk.zip-nhbJ.rar`

Downloaded 25 May 2012 to 156.111.111.124. Redistribution subject to AIP license or copyright; see http://proceedings.aip.org/about/rights_permissions

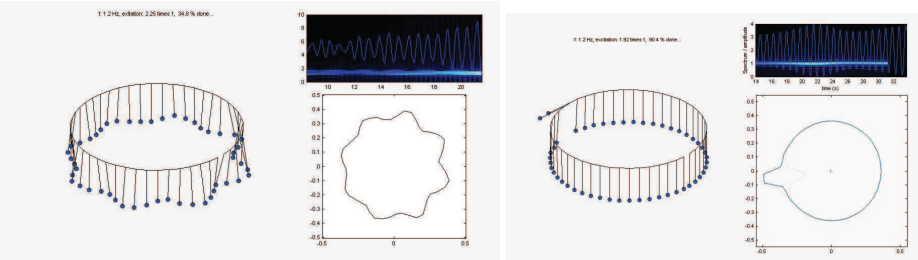


FIGURE 3. Spherical mode $Y_{l=8}^{(m)}$ observed when $f_0 = \frac{f_{ext}}{2.25}$. Modulational instability is observed in the time and frequency domain (top right curve). Localized mode observed at $f_0 = \frac{f_{ext}}{1.92}$ showing a trapping like behavior of energy. Modulation instability is observed in the time and frequency domain (top right curve)

bubble oscillation is then given by $\ddot{a}_l(t) + 2\gamma\dot{a}_l(t) + \omega_l^2 a_l(t) = 0$ where ω_l is given by $\omega_l^2 = (l-1)(l+1)(l+2)\frac{\sigma}{\rho R_0^3}$. The spherical mode is unstable, *i.e.* $R(t) \rightsquigarrow R(t,\theta)$, MI appears and localized behavior is observed (as shown in Fig.**??** when $\omega_{ext} = 1.92 f_0$. This model stand on the equation give by Marmottant [1] and the modification of $R(t)$ whose represents the radius distorsions in adding at this one an obtain value by the add of Spherical Harmonics. We have now $R(t)$ who becomes $R(t) + \sum a_n Y_n^m$. With a_n who is the distorsion amplitude and Y_n^m is Legendre Polynomial. After approximation like [7] and [8], we obtain a differential equation which corresponds to an harmonic oscillator who is writing like :

$$\ddot{a}_n(t) + 2\gamma\dot{a}_n(t) + \omega a_n(t) = 0 \tag{10}$$

With $\gamma = [3\frac{\dot{R}}{R} + 2(n+2)(2n+1)\frac{\mu}{\rho R^2}]$ And $\Omega = (n-1)[(n+1)(n+2)\frac{\sigma}{\rho R^3} - \frac{\ddot{R}}{R} + 2(n+2)\frac{\mu\dot{R}}{\rho R^3}]$ Of this result, we can have that when $R(t) \to R_0$, we find us with pulsation for surfaces modes like that :

$$\omega_n^2 = (n-1)(n+1)(n+2)\frac{\sigma}{\rho R_0^3} \tag{11}$$

CONCLUSION AND PERSPECTIVES

The perspective is to complete the Symmetry Analysis[2, 10, 11] method where all variables are studied thanks to a transformation by using the group G a one parameter a

$$G : \bar{S} = C^S(a)S + K^S(a), \tag{12}$$

where S denotes physical variables. The perspective of this analysis is to define practical optimized ultrasound pulses exciting the bubble and leading to drug delivery applications.

REFERENCES

1. P. Marmottant, S. van der Meer, M. Emmer, M. Versluis, N. de Jong, S. Hilgenfeldt, and D. Lohse, *Journal of the Acoustical Society of America* **118**, 3499–3505 (2005).
2. B. J. Cantwell, *Introduction to Symmetry Analysis*, Cambridge University Press (612 pages), 2002.
3. E. Kenig, B. A. Malomed, M. C. Cross, and R. Lifshitz, *Phys. Rev. E* **80**, 046202 (2009).
4. A. J. Sievers, and S. Takeno, *Phys. Rev. Lett.* **61**, 970–973 (1988).
5. D. Rabaud, P. Thibault, M. Mathieu, and P. Marmottant, *Phys. Rev. Lett.* **106**, 134501 (2011).
6. A. Maksimov, *Journal of Experimental and Theoretical Physics* **106**, 355–370 (2008).
7. U. H. Augsdörfer, A. K. Evans, and D. P. Oxley, *Physical Review* **61**, 5278–5286 (2000).
8. R. Nabergoj, and A. Francescutto, *Journal de Physique* **40**, 306–309 (1979).
9. V. J. Sánchez-Morcillo, I. Pérez-Arjona, V. Espinosa, M. Castro, and R. Sánchis-Ojeda, Estructuras dinámicas en cadenas de osciladores acoplados con forzamiento paramétrico (2009).
10. N. H. Ibragimov, and O. V. Rudenko, *Acoustical Physics* **50**, 406–419 (2004).
11. S. Dos Santos, and C. Plag, *Int. Journal of Non-Linear Mechanics* **43**, 164–169 (2008).

Downloaded 25 May 2012 to 156.111.111.124. Redistribution subject to AIP license or copyright; see http://proceedings.aip.org/about/rights_permissions